Visible light superoxide radical anion generation by tetra(4-carboxyphenyl)porphyrin/TiO$_2$: EPR characterization

Carlos E. Diaz-Uribe [a,b], Martha C. Daza [a,*], Fernando Martínez [b], Edgar A. Páez-Mozo [b], Carmen L.B. Guedes [c], Eduardo Di Mauro [c]

[a] Grupo de Bioquímica Teórica, Universidad Industrial de Santander, Bucaramanga, Colombia
[b] Centro de Investigaciones en Catálisis, Universidad Industrial de Santander, Bucaramanga, Colombia
[c] Laboratório de Fluorescência e Ressonância Paramagnética Eletrônica, LAFLURPE, Universidade Estadual de Londrina, Londrina, PR, Brazil

ARTICLE INFO

ABSTRACT

The generation of superoxide radical anion O$_2$$^{\bullet-}$ from tetra(4-carboxyphenyl)porphyrin (TCPP) adsorbed on TiO$_2$ in DMSO and irradiated by visible light was studied using EPR spectroscopy and 5,5-dimethyl-1-pyrroline-N-oxide (DMPO) as spin trap. A chemical filter was used to remove light with wave lengths <500 nm. A multiline EPR spectrum was observed, characteristic of a mixture of two adducts, the first corresponding to DMPO–O$_2$$^{\bullet-}$ and the second to the so-called nitroxide-like radical. Hyperfine coupling constants determined for the DMPO–O$_2$$^{\bullet-}$ adduct are: $a_N = 14.1$ G, $a_H^\beta = 10.8$ G and $a_H^\gamma = 1.4$ G, and for the nitroxide-like radical adduct $a_N = 14$ G. An increased intensity of the EPR lines corresponding to the nitroxide-like radical adduct was observed under irradiation without chemical filter, which suggests a possible DMPO–O$_2$$^{\bullet-}$ decomposition. No singlet oxygen could be detected by EPR spectroscopy using 2,2,6,6-tetramethyl-4-piperidone (TEMP) as spin trap and by chemical trapping using anthracene as the trap.

© 2010 Elsevier B.V. All rights reserved.

1. Introduction

The superoxide radical anion (O$_2$$^{\bullet-}$) plays a very important role in biological pathways and in complex chemical reactions [1–3]. It is generated in living cells in processes involving NADPH oxidases, mitochondrial electron transport, cytocrome P-450 reactions, and it is thought to be important in the radical theory of aging [4], gene expression in photosynthetically active chloroplasts [5], and in regulating plant growth [6]. The superoxide radical anion is relatively unstable in aqueous media and more reactive than oxygen, due to the unpaired electron in its π^* orbital. O$_2$$^{\bullet-}$ has a dual nature: it is a negatively charged species and it is a radical with one unpaired electron. It may react as a free radical or induce one-electron reduction or oxidation reactions.

The superoxide radical anion can be generated by: (a) dissolution of KO$_2$ in different organic solvents containing 18-crown-6 ether [7]; (b) UV photolysis of benzoxaprofen [8,9]; (c) UV radiation of TiO$_2$ [10]; (d) electrolysis of oxygen in aprotic solvents and electrochemical reduction of dioxygen [11–13]; (e) electron transfer from a photoexcited sensitizer to dissolved oxygen [14] and (f)

photoinduced electron transfer from thionine and eosin Y [15,16], ethyl ester of fluorescein [17], methylene blue, rhodamine B [18], hypocrellin [19] or porphyrins [20,21] to the conduction band (CB) of TiO$_2$.

In this work, in order to gain deeper insight into the generation and detection of O$_2$$^{\bullet-}$, we have investigated the visible light generation of O$_2$$^{\bullet-}$ with TiO$_2$ sensitized with tetra(4-carboxyphenyl)porphyrin (TCPP) (Fig. 1).

The sensitizer in its first singlet (S_1) and triplet (T_1) excited states can be obtained by absorption of UV/vis radiation from its ground state S_0. T_1 is yielded by the relaxation of S_1 through intersystem crossing. When photoreactivity is discussed, both S_1 and T_1 excited states have to be taken into account. The lifetime of T_1 is longer (ms) than S_1 (ns), allowing it to be more reactive. T_1 can react via type-I or type-II processes. The type I-process involves hydrogen atom abstraction or electron transfer between the excited sensitizer and the substrate, yielding free radicals. These radicals can react with oxygen to form the superoxide anion. The type-II process involves energy transfer from T_1 to molecular oxygen to produce singlet oxygen O$_2$ ($^1\Delta_g$). The type-I process can involve S_1 or T_1. However, due to the short lifetime of S_1, the sensitizer can only react in this state if it is intimately associated with a substrate. In both cases the interaction requires readily oxidizable or reducible substrates [22]. The type-I process has been observed in the sensitization of TiO$_2$ by different dyes [15–21], which occurs through excitation of
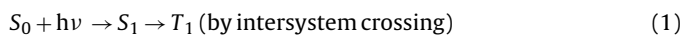
* Corresponding author at: Cra. 27 Calle 9 Ciudad Universitaria, Bucaramanga, Colombia. Tel.: +57 76346149.
E-mail addresses: marthacde@yahoo.com, mcdaza@uis.edu.co (M.C. Daza).
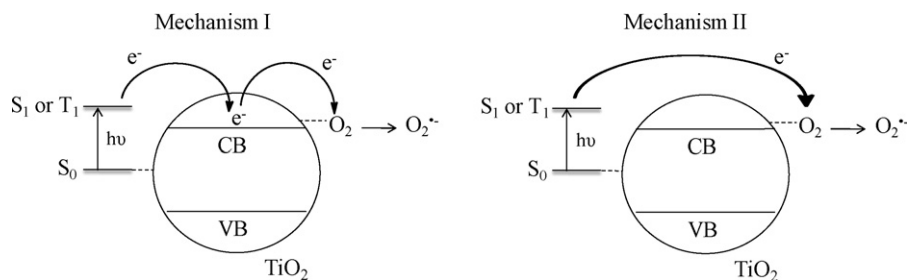
Scheme 1. Mechanism of superoxide anion generation. S_0 = sensitizer ground state, S_1 = singlet excited state, T_1 = triplet excited state, CB = conduction band, VB = valence band [20 (modified)].

the sensitizer followed by electron transfer to the TiO_2 conduction band (Eqs. (1)–(3)).

$$S_0 + h\nu \rightarrow S_1 \rightarrow T_1 \text{ (by intersystem crossing)} \quad (1)$$

$$S_1 \text{ or } T_1 + TiO_2 \rightarrow (S_1 \text{ or } T_1)^+ + TiO_2(e_{CB}{}^-) \quad (2)$$

$$TiO_2(e^-{}_{CB}) + O_2 \rightarrow TiO_2 + O_2{}^{\bullet -} \quad (3)$$

The superoxide anion can be formed by two different mechanisms according to Scheme 1. O_2 adsorbed on the TiO_2 surface can be reduced by an electron from the conduction band (mechanism I) or via electron transfer from S_1 or T_1 (mechanism II) to generate superoxide anion.

Superoxide anion can be detected by (a) luminol chemiluminescence probe [23], (b) superoxide dismutase inhibitable cytochrome c reduction method [24], and (c) EPR spectroscopy using 5,5-dimethyl-1-pyrroline-N-oxide (DMPO) as a spin trap [25], Scheme 2. It is possible to determine superoxide radical anion in both protic and aprotic solvents by EPR [11,17,19]. In ethanol the hyperfine coupling constants are not determined clearly due to the background noise [17,19]. On the other hand, the DMPO–OOH adduct can suffer rapid spontaneous transformation into DMPO–OH in aqueous media [26]. The generation of superoxide anion in aprotic solvents, such as DMSO is extremely useful because in this solvent the molecule is stable for several days, compared to seconds in aqueous solutions [27]. $O_2{}^{\bullet -}$ reacts with DMPO to form DMPO–$O_2{}^{\bullet -}$ [25]. DMPO can be directly oxidized to 5,5-dimethyl-1-pyrroline-N-oxide-N-oxyl (DMPOX) radical [28–30], or decomposed to a nitroxide-like radical by cleavage of the N–C bond and ring opening [31,32]. DMPO–$O_2{}^{\bullet -}$, DMPOX and the nitroxide-like radicals can be identified by their hyperfine coupling constants (hcc).

In this work, the production of DMPO–$O_2{}^{\bullet -}$ with TCPP/TiO_2 under visible light has been investigated and the formation of a nitroxide-like radical was observed. It has been shown that singlet oxygen was not detected.

2. Materials and methods

2.1. Materials

Solvents were purchased from J.T. Baker. 2,2,6,6-Tetramethyl-4-piperidone (TEMP) and 5,5-dimethyl-l-pyrroline-N-oxide (DMPO) were manufactured by Sigma–Aldrich. Superoxide dismutase was purchased from Aldrich. TiO_2 Degussa P-25 with a specific area of $50\,m^2\,g^{-1}$ corresponding to a particle size of ca. 30 nm was employed as support [33]. All reactives were of analytical grade.

2.2. Spectroscopic measurements

The UV–vis spectra of TCPP in ethanol were measured using a Hewlett-Packard 8453 spectrophotometer. The UV–vis diffuse reflectance absorption spectrum of solid TCPP/TiO_2 was measured using a Lambda 4 Perkin Elmer spectrophotometer equipped with an integrating sphere. FT-IR spectra (KBr) were recorded on a Bruker Tensor 27 spectrometer.

2.3. Synthesis of TCPP

Tetra(4-carboxyphenyl)porphyrin (TCPP) was synthesized according to the methods described in the literature [34,35]. Pyrrole (30 mmol) was added to a mixture of 4-carboxybenzaldehyde
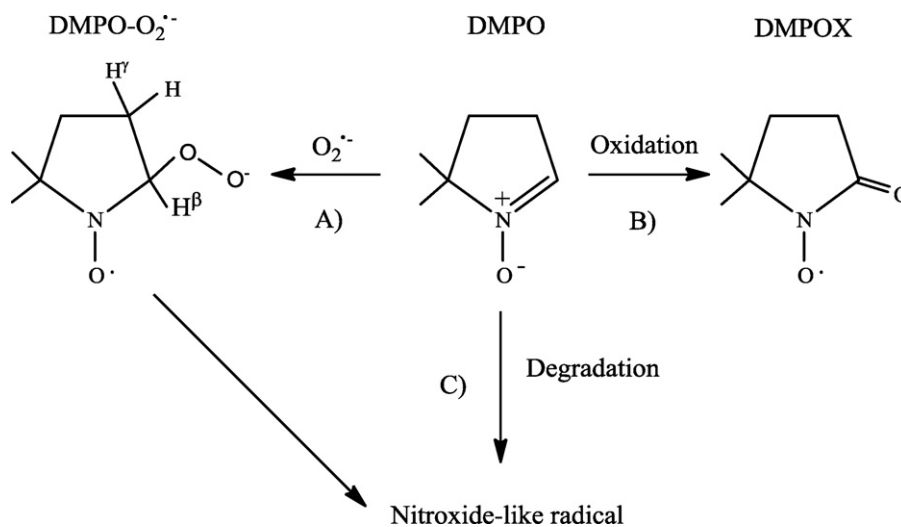
Scheme 2. (A) Reaction of 5,5-dimethyl-1-pyrroline-N-oxide, DMPO, with superoxide radical anion $O_2{}^{\bullet -}$, yielding a paramagnetic adduct DMPO–$O_2{}^{\bullet -}$. (B) Oxidation of DMPO yielding 5,5-dimethyl-1-pyrroline-N-oxide-N-oxyl (DMPOX) radical. (C) Degradation of DMPO to nitroxide-like radical.
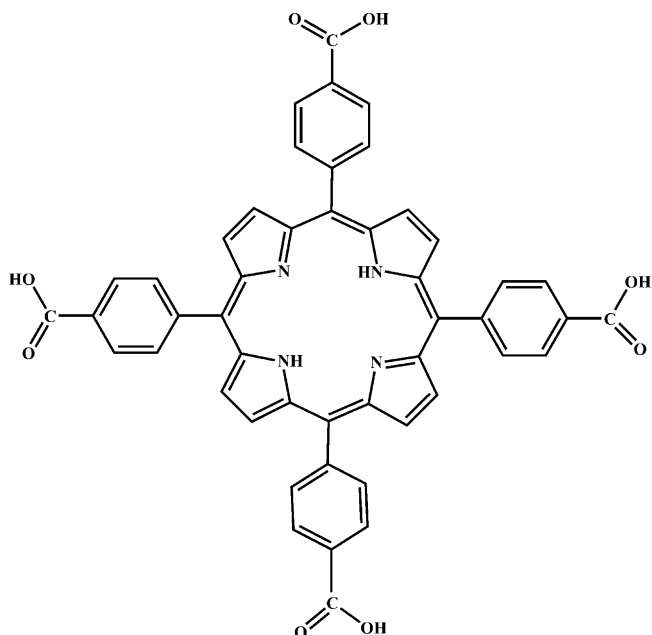
Fig. 1. Representation of tetra(4-carboxyphenyl)porphyrin (TCPP) structure.

(30 mmol), propionic acid (105 mL) and nitrobenzene (45 mL). The mixture was heated for 1 h at 120 °C. After cooling the solvent was removed under vacuum and the porphyrin was dissolved in 250 mL of 0.1 M NaOH. The porphyrin was precipitated with 1 M HCl solution, dissolved in ethanol and recrystallized by solvent evaporation.

2.4. Adsorption of TCPP on TiO$_2$

6.3 mmol of TiO$_2$ were suspended in 250 mL of 0.4 mM TCPP solution (pH >10) for 1 h. The mixture was stirred overnight at 60 °C. Afterwards, the pH was adjusted to 3.0 with 0.1N H$_2$SO$_4$, and the solid was filtered, washed with distilled water and dried at room temperature [36]. A sample of TCPP/TiO$_2$, treated with 0.1 M NaOH solution and extracted in ethanol, was examined by UV–vis spectroscopy.

2.5. EPR experiments

(a) *Superoxide radical anion formation applying the EPR-DMPO method* [25]

Generation of superoxide radical anion by visible light using TCPP/TiO$_2$ was examined by EPR spectroscopy signal of the DMPO–O$_2$$^{\bullet-}$ adduct. The formation of superoxide anion was measured in a suspension of 0.01 g of TCPP/TiO$_2$ in a solution of DMPO (50 mM) in DMSO. Photoreactions were carried out in an immersion well-type quartz photoreactor system supplied by Ace Glass-7880 (see Fig. 2). The solution was irradiated with visible light (halogen lamp of 100 W) filtered with a potassium dichromate solution (1 M) circulating in the immersion well (part (a) in Fig. 2) to remove wavelengths <500 nm. The samples were transferred immediately to 100 μL quartz capillaries and were measured under normal conditions, with 100 kHz magnetic field modulation, 10 mW microwave power and 5 G modulation amplitude in a JEOL (JES-PE-3X) spectrometer. Spectra were simulated using the BRUKER® WINEPR SimFonia Version 1.25 software to determine the spin Hamiltonian parameters of DMPO–O$_2$$^{\bullet-}$ and a nitroxide-like radical.

(b) *Singlet oxygen formation*

Photogenerated singlet oxygen reacts with TEMP yielding the paramagnetic TEMPO, which shows a characteristic three-line EPR
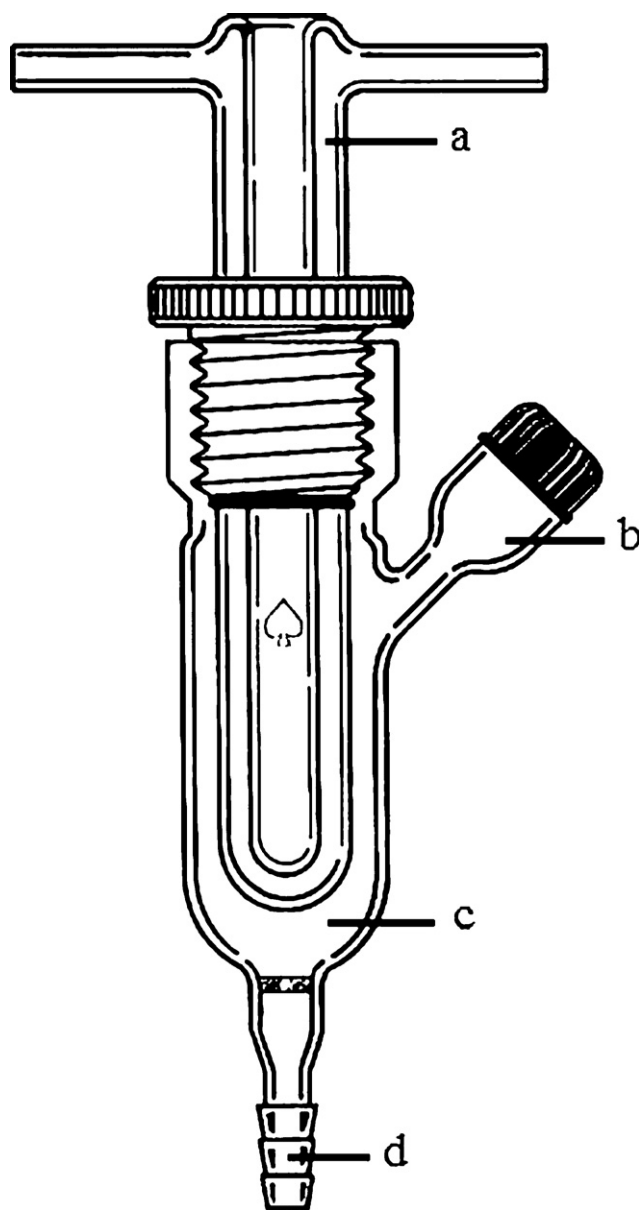

Fig. 2. Photoreactor: (a) immersion well; (b) sampling device; (c) reactor body and (d) gas inlet.

spectrum [37]. Singlet oxygen was detected in a suspension of 0.12 mmol of TCPP in a solution of TEMP (10 mM) in toluene, irradiated with visible light (halogen lamp of 100 W) filtered with a solution of potassium dichromate (1 M) to remove wavelengths <500 nm, same as described above. The samples in quartz tubes were measured under normal conditions, with 100 kHz magnetic field modulation, 10 mW microwave power and 5 G modulation amplitude in a JEOL (JES-PE-3X) spectrometer.

2.6. Singlet oxygen chemical trapping by anthracene

The experiments were performed in oxygen atmosphere, according to the following procedure: 0.12 mmol of the TCPP or TCPP/TiO$_2$ was added to 10 mL of a solution of anthracene dissolved in dichloromethane (0.2 mM), in a batch photo-reactor with a 100 W OSRAM halogen immersion lamp. The light was filtered through a 1 M potassium dichromate solution to remove wavelengths <500 nm (see above). Irradiation of the suspension was started after 1 h in the dark (with stirring). Sample aliquots of 0.1 mL
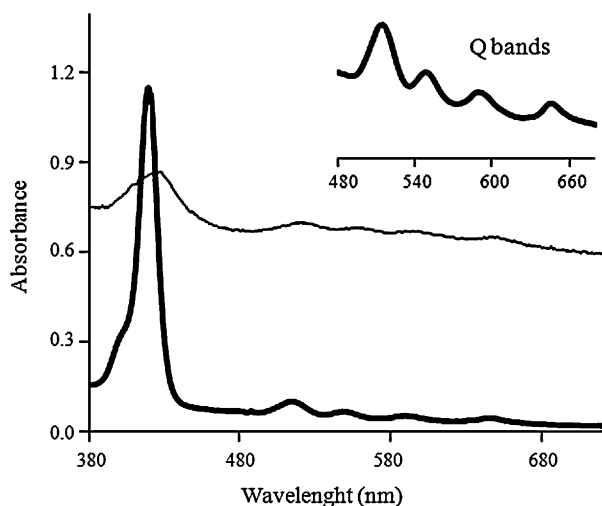
Fig. 3. UV–vis spectra of TCPP in ethanol solution (thick line) and TCPP adsorbed on TiO$_2$ (thin line).

Fig. 4. FT-IR spectra (KBr pellets) for metal-free TCPP and TCPP adsorbed on TiO$_2$ surface.

were taken during irradiation, filtered and measured by UV–vis spectrophotometry at λ_{max} = 375 nm.

A sample of the reaction mixture was analyzed by GC–MS in a 5890 Hewlett Packard gas chromatograph, with a 5972 mass selective detector and a HP5-MS (30 m long and 0.25 mm internal diameter) column and with He as the carrier gas (1 mL/min). 1 μL sample aliquots were injected with split (1:30). The following temperature program was applied: heating at 200 °C for 5 min, heating to 300 °C with a rate of 10 °C/min. This temperature was maintained for 15 min. Detector conditions: 70 eV, electronic impact, 35–400 m/z mass range, 200 V EM voltage (A-tune), 20 Hz Sweep Frequency at 230 °C.

3. Results and discussion

3.1. Characterization of TCPP and TCPP/TiO$_2$

UV–vis absorption spectra of the TCPP in ethanol showed a typical Soret band and four Q bands (Fig. 3). The band at 419 nm was assigned to the Soret band arising from the transition $a_{1u}(\pi)$–$e_g{}^*(\pi)$. The other four absorption maxima (514, 548, 588 and 645 nm) were attributed to the Q bands corresponding to the $a_{2u}(\pi)$–$e_g{}^*(\pi)$ transitions [38]. The absorption spectrum of TCPP adsorbed on TiO$_2$ particles is similar to the corresponding free porphyrin spectrum but exhibits a small 8 nm red shift. This is possibly due to electronic coupling between the π^* orbital of TCPP and the d orbital of TiO$_2$ due to the chemical linkage [39]. This coupling stabilizes the π^* orbital by delocalization, decreasing its energy, which explains the observed shift of the absorption bands [40]. The amount of TCPP adsorbed onto TiO$_2$ was found to be 0.4 g per 1 g of TCPP/TiO$_2$.

The FT-IR absorption spectra of TCPP free (a) and adsorbed on TiO$_2$ (b) are shown in Fig. 4. For free TCPP, the characteristic band of ν(C=O) of the carboxylic acid group is observed at around 1701 cm^{-1}. C–O stretching modes are observed at 1225 and 1268 cm^{-1} [41]. When TCPP is adsorbed on TiO$_2$, the C=O and C–O bands intensities decreased and the two intense bands at 1630 and 1381 cm^{-1} can be assigned to the antisymmetric and symmetric ν(–CO$_2{}^-$) modes, respectively. These bands and the disappearance of ν(C=O) reveal that carboxylic acid groups can be chemisorbed as carboxylates on the TiO$_2$ surface [39,42].

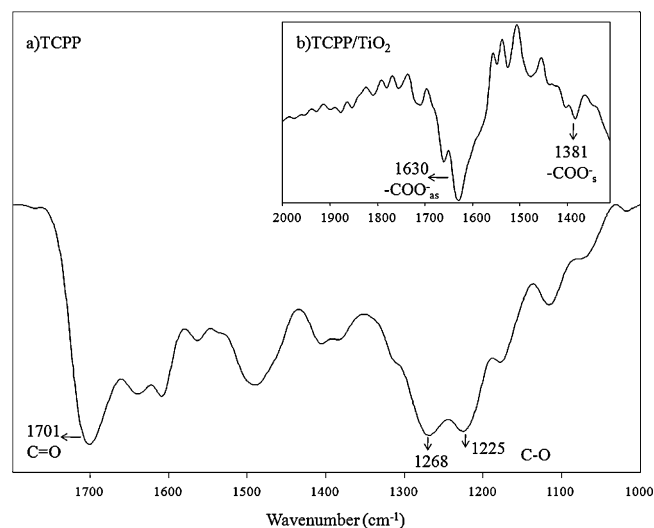### 3.2. Generation of superoxide radical anion and detection by EPR spin trapping

The ability of the photoexcited TCPP to transfer electrons to TiO$_2$ depends on the energy difference between the TiO$_2$ conduction band (CB) and the excited singlet state (oxidation potential) of the porphyrin. Fig. 5 shows the relative energy levels of the TiO$_2$ particles and the anchored TCPP. The redox potential of the singlet excited state ^{1}TCPP* is about -1.36 V vs NHE and the energy level of the conduction band of TiO$_2$ lies around -0.5 V vs NHE [43]. The reduction potential for oxygen to form the superoxide anion is -0.18 V [44], which is below the redox potential of ^{1}TCPP* and below the energy level of the conduction band of TiO$_2$. This renders the electron transfer process from the excited state of the porphyrin to the CB of TiO$_2$ and from here to O$_2$ thermodynamically possible. The adsorbed ^{1}TCPP* state injects an electron into the conduction band of TiO$_2$ and the electron can also be scavenged by adsorbed oxygen to give the superoxide radical anion [17,43].

TCPP/TiO$_2$ irradiated with visible light ($\lambda > 500$ nm) generates O$_2{}^{\bullet-}$ which, in the presence of DMPO, produces DMPO–O$_2{}^{\bullet-}$ radical characterized by a multiline EPR spectrum (Fig. 6b). This spectrum can be interpreted in terms of a mixture of two types of DMPO adducts, based on their hyperfine interactions (hf): the DMPO–O$_2{}^{\bullet-}$
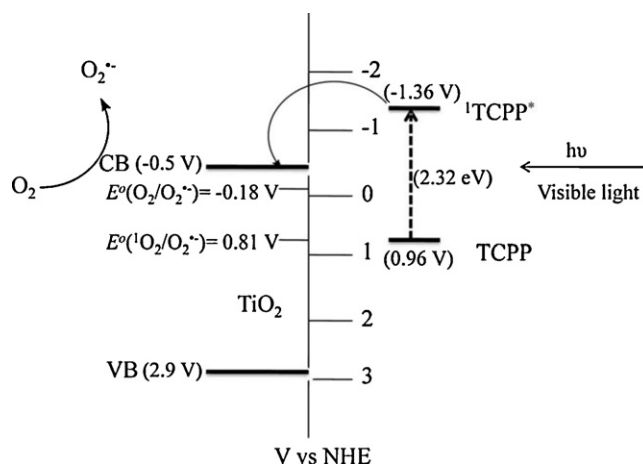

Fig. 5. Diagram illustrating the energetics of sensitation of TiO$_2$ particles by TCPP [43 (modified)].
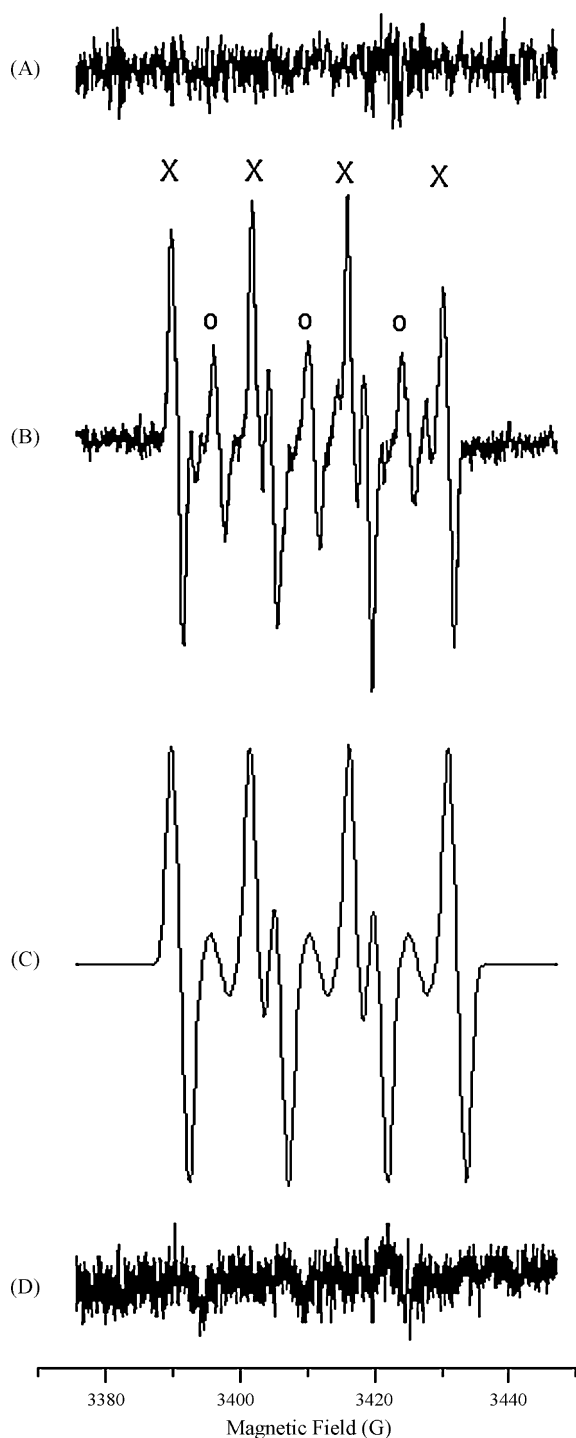
Fig. 6. EPR spectrum. (a) In the dark; (b) after 2 min under irradiation with visible light of the TCPP/TiO$_2$, DMPO–O$_2^{•−}$ (x) and nitroxide-like radical (o); (c) simulated signal obtained by the combination of two spin adducts; and (d) in presence of SOD.

with $a_N = 14.1$ G, $a_H^\beta = 10.8$ G and $a_H^\gamma = 1.4$ G and the nitroxide-like radical with $a_N = 14$ G. The EPR parameters are consistent with reported values for DMPO–O$_2^{•−}$ in dimethyl sulfoxide [9].

The EPR spectrum of these two adducts was simulated using the above hf values. When these two spectra were combined in the ratio 75:25 (DMPO–O$_2^{•−}$:nitroxide-like radical) the simulated signal (Fig. 6c) fitted well with the observed spectrum. No EPR signal was observed when pure DMPO was irradiated in DMSO or when the experiment was performed in the dark (Fig. 6a). Addition of superoxide dismutase (SOD) (50 μg/mL) prior to illumination
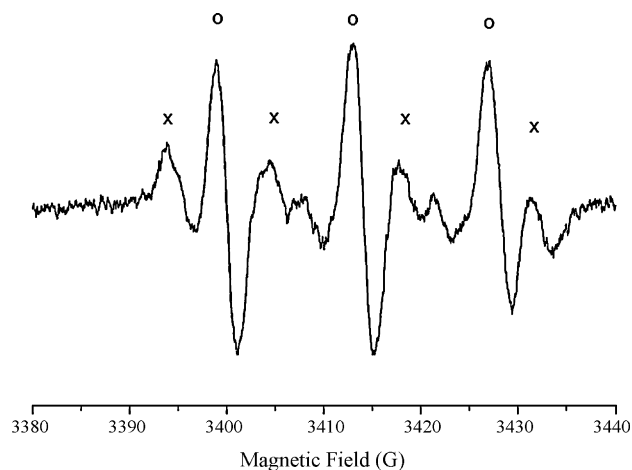

Fig. 7. EPR spectrum of DMPO–O$_2^{•−}$ adduct (x) and nitroxide-like radical (o).

inhibited the generation of spin adducts, in agreement with other authors [45,46], as shown in Fig. 6d, indicating that DMPO–O$_2^{•−}$ is the main product formed. The additional three-line signal with $a_N = 14$ G (showed with o) suggests that DMPO–O$_2^{•−}$ may later decompose to generate the nitroxide-like radical. This radical could be formed by cleavage of the N–C bond and ring opening of the DMPO–O$_2^{•−}$ [31,32].

Usually the DMPO–O$_2^{•−}$ EPR spectrum shows a splitting caused by the interaction of the unpaired electron with the nitrogen nucleus ($I = 1$) of the nitroxide. Further, a second splitting deriving from the unpaired electron interacting with the hydrogen nucleus H$^\beta$ ($I = 1/2$), and a third splitting deriving from the unpaired electron interacting with a secondary proton H$^\gamma$ ($I = 1/2$) are also observed. The generation of superoxide anion in aprotic solvents, such as DMSO is extremely useful because in this solvent the molecule is stable for several days, compared to seconds in aqueous solutions [27]. Furthermore, all DMPO–O$_2^{•−}$ hyperfine coupling constants are well resolved in DMSO. For example, in ethanol using hypocre-llin B/TiO$_2$ it was only possible to determine the hyperfine coupling constant a_N [19] and in fluorescein ethyl ester the hyperfine coupling constant a_H^γ could not be determined [17].

The formation of nitroxide-like radical may be due to light-induced decomposition of the unstable DMPO–O$_2^{•−}$ adduct. Fig. 7 shows a different EPR spectrum of O$_2^{•−}$ produced from TCPP/TiO$_2$ under irradiation without chemical filters. The intensity of the three lines related to the nitroxide-like adduct increases when irradiated without a chemical filter. This suggests a decomposition of the adduct DMPO–O$_2^{•−}$ induced by UV light. The simulated EPR spectrum fits the experimental spectrum when the signal of DMPO–O$_2^{•−}$ and nitroxide-like radical were combined in a ratio of 20:80. For the nitroxide-like radical, the interaction of the unpaired electron with the nitrogen nucleus ($I = 1$) results in a spectrum with three lines with a hyperfine splitting constant of 14 G.

Control experiments with bubbling air and pure oxygen showed the formation of the adduct DMPO–O$_2^{•−}$. In experiments of Carmichael, using adriamycin and daunomycin, formation of the DMPO–O$_2^{•−}$ adduct was not observed when the experiment was performed under bubbling with N$_2$ [47]. He et al. using fluorescein/TiO$_2$ in ethanol under visible light irradiation, could not detect reactive oxygen species by EPR in absence of O$_2$ [17].

Because TCPP is highly soluble in DMSO, and the impossibility to resolve the EPR spectra of TCPP and DMPO–O$_2^{•−}$ adducts, we evaluated the superoxide anion generation using TCPP adsorbed on inert SiO$_2$ under the same conditions [48]. We did this to define the mechanism of superoxide anion generation. The absence of a DMPO–O$_2^{•−}$ signal suggests that electron transfer from the S_1 sin-
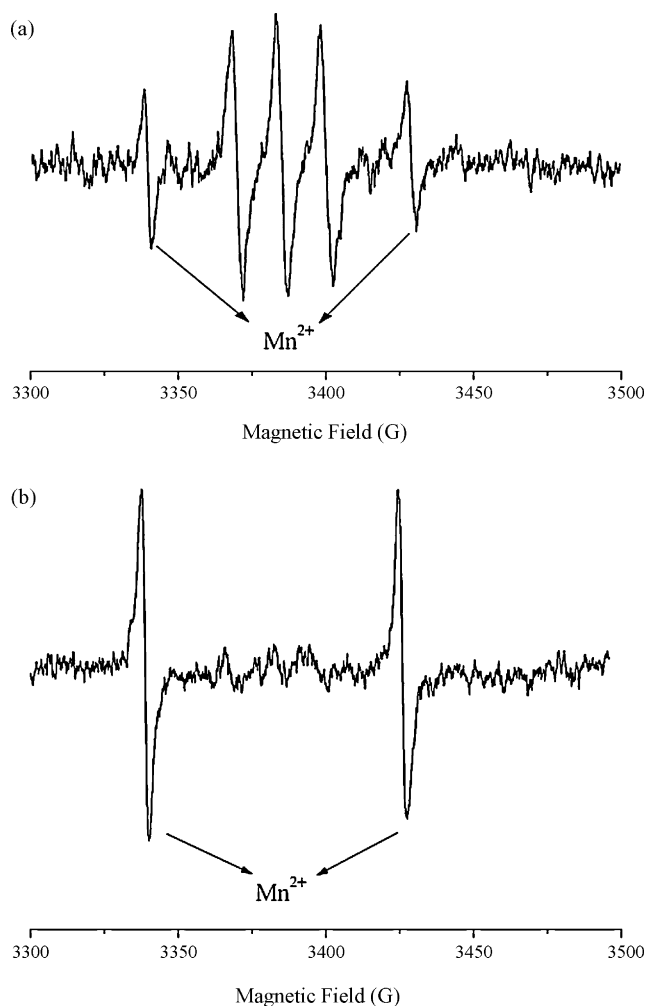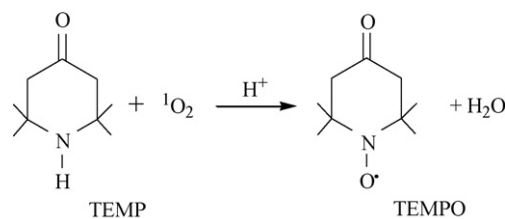
Fig. 8. EPR spectrum at room temperature of the TEMPO after 2 min of irradiation, (a) TCPP (b) TCPP/TiO$_2$. MgO:Mn^{2+} was used as a g marker.

Scheme 3. Formations of TEMPO adduct.

glet or T_1 triplet excited state of TCPP to O$_2$ is insignificant and can be neglected. These results allow us to suggest that superoxide anion generation by TCPP/TiO$_2$ in DMSO occurs through mechanism I (Scheme 1). O$_2$$^{•−}$ generation by the same mechanism in protic solvents was demonstrated recently by Xu et al. [19] using hypocrellin/TiO$_2$ and He et al. [17] using ethyl ester of fluorescein/TiO$_2$ in ethanolic media. O$_2$$^{•−}$ can be produced via mechanism II too, as was shown recently by Yu et al. [20] using a derivative of anisyltritolylporphyrin (ATTP)/TiO$_2$ terminated with bromo group and carboxyl, and by both mechanisms (Scheme 1) using ATTP terminated with tyrosine methyl ester [20].

3.3. Detection of singlet oxygen by EPR spin trapping and chemical trapping by anthracene

In order to study the generation of singlet oxygen from TCPP and TCPP/TiO$_2$, the EPR spin trapping technique was applied with TEMP as spin trap. An EPR spectrum consisting of three equally intense lines was observed when a solution with TCPP was irradiated with visible light at room temperature (Fig. 8). This spectrum is characteristic of TEMPO ($g = 2.006$ and $a_N = 15.5$ G) [49]. The formation of TEMPO is due to the oxidation of TEMP by singlet oxygen, as shown in Scheme 3. With TCPP/TiO$_2$ using the EPR method the TEMPO signal was not detected. This can be interpreted in different ways: first, it is difficult to detect ^{1}O$_2$ in heterogeneous systems. We have observed this effect in our study on TCPP and TCPP/SiO$_2$, where the

TEMPO signal was reduced (~50%) in TCPP/SiO$_2$ compared to free TCPP [48]. Similar results were obtained by Wang et al. [50].

Second, the singlet oxygen quantum yield of TCPP supported on TiO$_2$ could be reduced due to the C–O–Ti bonds between sensitizer and TiO$_2$ [39]. The carboxylate group enhances the electronic coupling between the π^* orbitals of the porphyrin and the Ti(3d) orbital manifold of TiO$_2$. This coupling leads to increased delocalization of the π^* level of the porphyrin and an efficient quenching of the excited singlet state of the sensitizer by TiO$_2$. As a consequence, less ^{1}O$_2$ would be produced by energy transfer from the T_1 state of the sensitizer [51]. Recently, singlet oxygen quantum yields between 0.20 and 0.25 were observed in TCPP/TiO$_2$, compared to 0.53 in homogeneous free TCPP [52]. Third, it might also be possible that ^{1}O$_2$ is reduced by electron transfer from the CB of TiO$_2$ generating superoxide anion as was suggested recently [50]. Thermodynamically this reaction is possible, because the redox potential (vs NHE) of ^{1}O$_2$/O$_2$$^{•−}$ is 0.81 V [44] which is below the redox potential of the conduction band of TiO$_2$ (see Fig. 5).

Chemical trapping by polycyclic aromatic hydrocarbons is specific for singlet oxygen and can be much more sensitive than the luminescence technique [53]. The [4 + 2] cycloaddition of singlet oxygen to conjugated cyclic dienes and polycyclic aromatic hydrocarbons is its most characteristic reaction. One of these polycyclic aromatic hydrocarbons, anthracene, exhibits two useful properties: (1) it reversibly traps singlet oxygen, and (2) its 9-hydroxy and 9-ketoanthracene reaction products indicate the presence of radicals in the reaction medium [54,55]. In the presence of anthracene and TCPP/TiO$_2$ no reaction product was found by GC–MS.

4. Conclusion

TCPP adsorbed on TiO$_2$ and dispersed in DMSO generates the superoxide radical anion in the presence of molecular oxygen and visible light. The DMPO–O$_2$$^{•−}$ adduct decomposes under irradiation with light and gives two products which have been identified by EPR. Hyperfine coupling constants have been determined for DMPO–O$_2$$^{•−}$ ($a_N = 14.1$ G, $a_H$$^\beta$ = 10.8 G and $a_H$$^\gamma$ = 1.4 G), and its decomposition product, a nitroxide-like radical ($a_N = 14$ G). The sum of the simulated signals of the two adducts reproduces the experimentally observed spectrum, confirming the generation of superoxide radical anion. No signals of the adduct between ^{1}O$_2$ and TEMP have been found in the EPR spectrum. However, this does not completely exclude the production of singlet oxygen, due to the difficulties to detect it in heterogeneous systems and the thermodynamically possible reaction of ^{1}O$_2$ with electrons of the conduction band of TiO$_2$.

Acknowledgments

References

[1] M.M. Tarpey, I. Fridovich, Methods of detection of vascular reactive species: nitric oxide, superoxide, hydrogen peroxide, and peroxynitrite, Circ. Res. 89 (2001) 224–236.

[2] M.E. Kerr, E.J. Monti, An introduction to oxygen free radicals, Heart Lung 25 (1996) 200–208.

[3] D. Parkinson, Oxygen free radicals: in search of a unifying theory of disease, Crit. Care Nurs. 11 (1995) 336–340.

[4] I. Afanas'ev, Superoxide Ion Chemistry and Biological Implications, CRC Press, USA, 1989.

[5] T.E. Scarpeci, M.I. Zanor, N. Carrillo, B. Mueller-Roeber, E.M. Valle, Generation of superoxide anion in chloroplasts of Arabidopsis thaliana during active photosynthesis: a focus on rapidly induced genes, Plant Mol. Biol. 66 (4) (2008) 361–378.

[6] K. Mi-Sun, K. Hyun-Soon, K. Yoon-Shik, B. Kwang-Hyun, O. Hyun-Woo, H. Kyu-Woong, B. Ro-Na, L. In-Jung, J. Hyouk, J. Jae-Heung, Superoxide anion regulates plant growth and tuber development of potato, Plant Cell Rep. 26 (2007) 1717–1725.

[7] S. Kim, R. DiCoslmo, J. San Filippo, Spectrometric and chemical characterization of superoxide, Anal. Chem. 51 (1979) 679–681.

[8] J.R. Harbour, L.M. Hair, Transient radicals in heterogeneous systems: Detection by spin trapping, Adv. Colloid Interface Sci. 24 (1985) 103–141.

[9] J.R. Harbour, L.M. Hair, Detection of superoxide ions in nonaqueous media: generation by photolysis of pigment dispersions, J. Phys. Chem. 82 (1978) 1397–1399.

[10] R. Konaka, E. Kasahara, W.C. Dunlap, Y. Yamamoto, K.C. Chien, M. Inoue, Irradiation of titanium dioxide generates both singlet oxygen and superoxide anion, Free Radic. Biol. Med. 27 (1999) 294–300.

[11] P. Pieta, A. Petra, W. Kutner, L. Dunsch, In situ ESR spectroscopic evidence of the spin-trapped superoxide radical, $O_2^{\bullet-}$, electrochemically generated in DMSO at room temperature, Electrochim. Acta. 53 (2008) 3412–3415.

[12] M.E. Peover, B.S. White, The formation of the superoxide ion by electrolysis of oxygen in aprotic solvents, Chem. Commun. 10 (1965) 183–184.

[13] P.S. Singh, D.H. Evans, Study of the electrochemical reduction of dioxygen in acetonitrile in the presence of weak acids, J. Phys. Chem. B. 110 (2006) 637–644.

[14] C. Hadjur, G. Wagniéres, F. Ihringer, Ph. Monnier, H. Van Der Bergh, Production of the free radicals $O_2^{\bullet-}$ and OH by irradiation of the photosensitizer zinc(II) phtalocyanine, J. Photochem. Photobiol. B: Biol. 38 (1997) 192–202.

[15] D. Chatterjee, A. Mahata, Evidence of superoxide radical formation in the photodegradation of pesticide on the dye modified TiO₂ surface using visible light, J. Photochem. Photobiol. A: Chem. 165 (2004) 19–23.

[16] D. Chatterjee, A. Mahata, Demineralization of organic pollutants on the dye modified TiO₂ semiconductor particulate system using visible light, Appl. Catal. B: Environ. 33 (2001) 119–125.

[17] J. He, J. Zhao, H. Hidaka, N. Serpone, EPR characteristics of a dye/colloidal TiO₂ system under visible light irradiation, J. Chem. Soc., Faraday Trans. 94 (1998) 2375–2378.

[18] D. Chatterjee, A. Mahata, Visible light induced photodegradation of organic pollutantson dye adsorbed TiO₂ surface, J. Photochem. Photobiol. A: Chem. 153 (2002) 199–204.

[19] S. Xu, J. Shen, S. Chen, M. Zhang, T. Shen, Active oxygen species ($^1O_2$, $O_2^{\bullet-}$) generation in the system of TiO₂ colloid sensitized by hypocrellin B, J. Photochem. Photobiol B: Biol. 67 (2002) 64–70.

[20] J. Yu, J. Chen, C. Li, X. Wang, H. Ding, ESR signal of superoxide radical anion adsorbed on TiO₂ generated at room temperature, J. Phys. Chem. B. 108 (2004) 2781–2783.

[21] W.M. Campbell, A.K. Burrell, D.L. Officer, K.W. Jolley, Porphyrins as light harvesters in the dye-sensitised TiO₂ solar cell, Coord. Chem. Rev. 248 (2004) 1363–1379.

[22] C.S. Foote, Definition of type I and type II photosensitized oxidation, Photochem. Photobiol. 54 (1991) 659.

[23] Y. Nosaka, Y. Yamashita, H. Fukuyama, Application of chemiluminescent probe to monitoring superoxide radicals and hydrogen peroxide in TiO₂ photocatalysis, J. Phys. Chem. B. 101 (1997) 5822–5827.

[24] W.H. Koppenol, J. Butler, The radiation chemistry of cytochrome c, Isr. J. Chem. 24 (1984) 11–16.

[25] J.R. Harbour, V. Chow, J.R. Bolton, An electron spin resonance study of the spin adducts of OH and HO₂ radicals with nitrone in ultraviolet photolysis of aqueous hydrogen peroxide solutions, Can. J. Chem. 52 (1974) 3549–3553.

[26] E. Finkelstein, G.M. Rosen, E.J. Rauckman, Production of hydroxyl radical by decomposition of superoxide spin-trapped adducts, Mol. Pharmacol. 21 (1982) 262–265.

[27] K. Ergaieg, M. Chevanne, J. Cillard, R. Seux, Involvement of both Type I and Type II mechanisms in Gram-positive and Gram-negative bacteria photosensitization by a meso-substituted cationic porphyrin, Sol. Energy 82 (2008) 1107–1117.

[28] R.A. Floyd, L.M. Soong, Spin trapping in biological systems oxidation of the spin trap 5,5-dimethyl-l-pyrroline- 1-oxide by a hydroperoxide-hematin system, Biochem. Biophys. Res. Commun. 74 (1977) 79–84.

[29] E.C. Evans, S.K. Jackson, C.C. Rowlan, An electron spin resonance study of radicals from chloramine-T-1, Tetrahedron 41 (1985) 5191–5194.

[30] S.D. Stan, J.S. Woods, M.A. Daeschel, Investigation of the presence of OH radicals in electrolyzed NaCl solution by electron spin resonance spectroscopy, J. Agric. Food Chem. 53 (2005) 4901–4905.

[31] A. Bosnjakovic, S. Shulamith, Spin trapping by 5,5-dimethylpyrroline-N-oxide in Fenton media in the presence of nafion perfluorinated membranes: limitations and potential, J. Phys. Chem. B. 110 (2006) 10720–10728.

[32] J.M. Lázaro-Martínez, M.F. Leal-Denis, L.L. Piehl, E. Rubín de Celis, G.Y. Buldain, V.C. Dall'-Orto, Studies on the activation of hydrogen peroxide for color removal in the presence of a new Cu(II)-polyampholyte heterogeneous catalyst, Appl. Catal. B: Environ. 82 (2008) 273–283.

[33] S. Cherian, C.C. Wamser, Adsorption and photoactivity of tetra(4-carboxyphenyl)porphyrin (TCPP) on nanoparticulate TiO₂, J. Phys. Chem. B. 104 (2000) 3624–3629.

[34] A.D. Adler, F.R. Longo, J.D. Finarelli, J. Goldmacher, J. Assour, L. Korsakoff, A simplified synthesis for meso-tetraphenylporphyrin, J. Org. Chem. 32 (1967) 476–1476.

[35] M.A. Schiavon, L.S. Iwamoto, A.G. Ferreira, Y. Iamamoto, M.V.B. Zanoni, D.M. Assis, Synthesis and characterization of a novel series of meso(nitrophenyl) and meso(carboxyphenyl) substituted porphyrins, J. Braz. Chem. Soc. 11 (2000) 458–466.

[36] G. Granados-Oliveros, E.A. Páez-Mozo, F. Martínez, C. Ferronato, J.M. Chevelon, Degradation of atrazine using metalloporphyrins supported on TiO₂ under visible light irradiation, Appl. Catal. B: Environ. 89 (2009) 448–454.

[37] Y. Lion, M.A. Delmelle, Van de Vorst, New method of detecting singlet oxygen production, Nature 263 (1976) 442–443.

[38] M. Gouterman, G.H. Wagnière, L.C. Snyder, Spectra of porphyrins. Part II. Four orbital model, J. Mol. Spectrosc. 11 (1963) 108–127.

[39] T. Ma, K. Inoue, H. Noma, K. Yao, E. Abe, Effect of functional group on photochemical properties and photosensitization of TiO₂ electrode sensitized by porphyrin derivatives, J. Photochem. Photobiol. A: Chem. 152 (2002) 207–212.

[40] G. Granados-Oliveros, F. Martínez-Ortega, E. Páez-Mozo, C. Ferronato, J.M. Chovelon, Photoactivity of metal-phenylporphyrins adsorbed on TiO₂ under visible light radiation: influence of central metal, The Open Mater. Sci. J. 4 (2010) 15–22.

[41] C. Wang, G.M. Yang, J. Li, G. Mele, R. Slota, M.A. Broda, M.Y. Duan, G. Vasapollo, X. Zhang, F.X. Zhang, Novel meso-substituted porphyrins: synthesis, characterization and photocatalytic activity of their TiO₂-based composites, Dyes Pigments 80 (2009) 321–328.

[42] T Hannappel, B. Burfeindt, W. Storck, F. Willig, Measurement of ultrafast photoinduced electron transfer from chemically anchored Ru-dye molecule into empty electronic states in a colloidal anatase TiO₂ film, J. Phys. Chem. B. 101 (1997) 6799–6802.

[43] R. Renganathan, A. Kathiravan, Effect of anchoring group on the photosensitization of colloidal TiO₂ nanoparticles with porphyrins, J. Colloid Interf. Sci. 331 (2009) 401–407.

[44] W.H. Koppenol, D.M. Stanbury, P.L. Bounds, Electrode potentials of partially reduced oxygen species, from dioxygen to water, Free Radic. Biol. Med. 49 (2010) 317–322.

[45] K.K. Mothilal, J.J. Inbaraj, C.F. Chignell, R. Gandhidasan, R. Murugesan, Photosensitisation with naphthoquinones and binaphthoquinones: EPR spin trapping and optical studies-formation of semiquinone radical and reactive oxygen species on photoillumination, J. Photochem. Photobiol. A: Chem. 163 (2004) 141–148.

[46] M. Rajendran, J.J. Inbaraj, R. Gandhidasan, R. Murugesan, Photogeneration of reactive oxygen species by 3-arylcoumarin and flavanocoumarin derivatives, J. Photochem. Photobiol. A: Chem. 182 (2006) 67–74.

[47] A.J. Carmichael, M.M. Mossoba, P. Riesz, Photogeneration of superoxide by adriamycin and daunomycin: An electron spin resonance and spin trapping study, FENS Lett. 164 (1983) 401–405.

[48] C.E. Diaz-Uribe, M.C. Daza, F. Martínez, E.A. Páez-Mozo, C.L. Guedes, E. Di Mauro, Singlet oxygen production by free tetra(4-carboxyphenyl)porphyrin-M (M = H, Cu and Zn) and tetra(4-carboxyphenyl)porphyrin/SiO₂. EPR and chemical trapping study, in preparation.

[49] C. Hadjur, A. Jeunet, P. Jardon, Photosensitization by hypericin: electron spin resonance (ESR) evidence for the formation of singlet oxygen and superoxide anion radicals in an in vitro model, J. Photochem. Photobiol. B: Biol. 26 (1994) 67–74.

[50] C. Wang, J. Li, G. Mele, G.M. Yang, F.-X. Zhang, L. Palmisano, G. Vasapollo, Efficient degradation of 4-nitrophenol by using functionalized porphyrin-TiO₂ photocatalysts under visible irradiation, Appl. Catal. B: Environ. 76 (2007) 218–226.

[51] Md.K. Nazeeruddin, R. Humphry-Baker, M. Gratzel, D. Wohrle, G. Schnurpfeil, G. Schneider, A. Hirth, N. Trombach, Efficient near-IR sensitization of nanocrystalline TiO₂ films by zinc and aluminum phthalocyanines, J. Porphyrin Phthalocyanines 3 (1999) 230–237.

[52] W. Li, N. Gandra, E.D. Ellis, S. Courtney, S. Li, E. Butler, R. Gao, pH-responsive TiO₂-attached porphyrin for singlet oxygen production in an aqueous solution, Appl. Mater. Interf. 1 (2009) 1778–1784.

[53] J.M. Aubry, C. Pierlot, J. Rigaudy, R. Schmidt, Reversible binding of oxygen to aromatic compounds, Acc. Chem. Res. 36 (2003) 668–675.

[54] D. Madhavan, K. Pitchumani, Photoreactions in clay media: singlet oxygen oxidation of electron-rich substrates mediated by clay-bound dyes, J. Photochem. Photobiol. A: Chem. 153 (2002) 205–208.

[55] F. Goulay, C. Rebrion-Rowe, J.L. Le Garrec, S.D. Le Picard, A. Casona, B.R. Rowe, The reaction of anthracene with OH radicals: An experimental study of the kinetics between 58 and 470 K, J. Phys. Chem. 122 (2005) 104308(1)–104308(7).